Radiocarbon, Vol 61, Nr 2, 2019, p 461–472 DOI:10.1017/RDC.2018.100

RADIOCARBON IN THE MARITIME AIR AND SEA SURFACE WATER OF THE SOUTH CHINA SEA

Pan Gao[1*] • Liping Zhou[1,2,3*] • Kexin Liu[4] • Xiaomei Xu[5]

[1]Key Laboratory for Earth Surface Processes, Department of Geography, Peking University, Beijing 100871, China.
[2]Institute of Ocean Research, Peking University, Beijing 100871, China.
[3]Laboratory for Marine Ecology and Environmental Science, Qingdao National Laboratory for Marine Science and Technology, Qingdao 266071, China.
[4]Institute of Heavy Ion Physics & State Key Laboratory of Nuclear Physics and Technology, Peking University, Beijing 100871, China.
[5]Keck Carbon Cycle AMS Laboratory, Department of Earth System Science, University of California, Irvine, CA 92697-3100, USA.

ABSTRACT. Radiocarbon (^{14}C) generated by the thermonuclear tests in the late 1950s to early 1960s has been used as a tracer to study atmospheric and oceanic circulations, carbon exchange between different reservoirs, and fossil fuel emissions. Here we report the first measurements of ^{14}C in atmospheric CO_2 of maritime air collected over the South China Sea (SCS) during July 2014. We also present ^{14}C of the dissolved inorganic carbon (DIC) in the sea surface water in the same region. Most of the $\Delta^{14}C$ values of the atmospheric CO_2 vary in the range of $15.6 \pm 1.6‰$–$22.0 \pm 1.6‰$, indicating that the central SCS maritime air is well-mixed and consistent with the clean background air in the Northern Hemisphere. The ^{14}C values of the DIC ($DI^{14}C$) in the surface seawater vary between $28.3 \pm 2.5‰$ and $40.6 \pm 2.7‰$, mainly due to the lateral mixing between the SCS and western Pacific. The average surface seawater $DI^{14}C$ is $15.4 \pm 5.1‰$ *higher* than that of the maritime air $^{14}CO_2$. The reversal of the sea–air $\Delta^{14}C$ gradient occurred at ~2000, marking the start of the upper ocean transferring bomb ^{14}C back to the atmosphere in the SCS.

KEYWORDS: $\Delta^{14}C$, bomb radiocarbon, dissolved inorganic carbon, maritime air CO_2, South China Sea.

INTRODUCTION

The anthropogenic addition to the radiocarbon (^{14}C) inventory has caused immense perturbation to the distribution of naturally produced ^{14}C, but provided a valuable tracer for study of the exchange of carbon between different reservoirs. Since the Nuclear Test-Ban Treaty in 1963, the concentration of bomb-produced ^{14}C in the atmosphere has decreased exponentially through the exchanges with the ocean and the terrestrial/biosphere reservoirs and by dilution with CO_2 derived from fossil fuel burning (Levin and Kromer 2004). The upper ocean has absorbed a large amount of bomb ^{14}C through air–sea exchange such that the average ^{14}C of the global surface ocean peaked in approximately 1973, about 10 years following the atmospheric bomb ^{14}C peak in the mid latitude Pacific Ocean (Druffel and Griffin 1995). Since the 1980s, the low- and mid-latitude oceans around ± 30° N and S have reached isotopic equilibrium with the decreasing atmospheric ^{14}C level (Caldeira et al. 1998).

The bomb ^{14}C pulse and subsequent decline have been used to constrain the global mean CO_2 exchange velocity and assess the ocean circulation processes that regulate oceanic uptake and storage of anthropogenic CO_2 (Broecker et al. 1985; Toggweiler et al. 1989; Krakauer et al. 2006; Sweeney et al. 2007; Graven et al. 2012). In contrast to the high-precision atmospheric bomb ^{14}C records on land (Levin and Kromer 2004; Turnbull et al. 2007; Levin et al. 2013), very limited data have been obtained on maritime air samples over the oceans (Bhushan et al. 1997; Dutta 2002; Kitagawa et al. 2004; Dutta et al. 2006). In a series of air–sea CO_2 exchange studies in the Northern Indian Ocean, Bhushan et al. (1997) and Dutta et al. (2006) measured tropospheric ^{14}C in the maritime air over the Arabian Sea and the Bay of Bengal. They showed that the $^{14}CO_2$ over this region decreased from $120 \pm 3‰$ in 1993 to $85 \pm 2‰$ in 2001. Kitagawa et al. (2004) reported tropospheric ^{14}C of a Japan-Australia transect over the

*Corresponding authors. Emails: pangao@pku.edu.cn; lpzhou@pku.edu.cn.

western Pacific during 1994–2002 and revealed a similar decreasing trend of maritime air $^{14}CO_2$ as in the remote background monitoring sites on land during the past decades.

The South China Sea (SCS) is the largest marginal sea in the western Pacific. The region is under strong influence of Asian monsoon, characterized by prevailing northeasterly winds in winter and southwesterly winds in summer. Driven by the seasonally reversed monsoon winds, the general circulation in the SCS upper layer is cyclonic in winter and anticyclonic in summer, respectively (Wyrtki 1961; Shaw and Chao 1994; Qu 2000a; Su 2004; Gan et al. 2006; Fang et al. 2009). Intrusions of Kuroshio Current through the Luzon Strait and mesoscale variability induced by eddies are also important features in the northeastern SCS (Qu et al. 2000b; Centurioni et al. 2004; Nan et al. 2015), which add complexity for the surface water circulation as well as for the oceanic exchange with atmosphere. Several studies have been conducted to assess the sea–air CO_2 fluxes in the SCS and shown that most areas of the SCS served as weak to moderate sources of CO_2 to the atmosphere (Dai et al. 2013; Zhai et al. 2013). However, no records of maritime air $^{14}CO_2$ and sea surface water DI^{14}C have been documented in the SCS. There were only four middle-deep depth (420–4170 m) seawater DI^{14}C data measured by Broecker et al. (1986) at one station in the central SCS. In this study, we measured ^{14}C in CO_2 of the maritime air collected over the SCS and ^{14}C of the DIC in the sea surface water (~5 m depth) in the same region. It is hoped that these measurements could have potentially important implications on the estimate of the air-sea CO_2 exchange and ocean circulation processes in this region.

MATERIAL AND METHODS

Air and Seawater Sampling

Maritime air and surface seawater samples were collected onboard the R/V *Dongfanghong 2* during a scientific investigation cruise in 2014, as part of the South China Sea Deep Processes project of the National Natural Science Foundation of China.

Ten maritime air samples were collected in the SCS open ocean area (>100 km from the shore) on July 6-15, 2014, and the last one was collected on the northeastern continental shelf of the SCS (~200 km from Xiamen) by the third leg of the cruise on July 6–17, 2014. The sampling sites are plotted in Figure 1 and the weather conditions for each sample are listed in Table 1. About 3.3 L of maritime air was sucked directly into a pre-evacuated stainless steel canister for about 1 min until it reached atmospheric pressure. The sampling location was located on the top deck of the vessel (about 10 m above sea level). In order to avoid any contamination from ship exhaust, air samples were collected during cruising after it left the seawater sampling site. Thus, the air and seawater sampling sites were not completely overlapping, but coupled in the best way feasible. Wind speed (m/s) and wind direction (meteorological convention, 0º = wind comes from the north) were obtained from the shipboard meteorological instrument.

During the 2nd and 3rd legs of the cruise between June 20 and July 14, 10 surface seawater samples were collected with the Carousel Water Sampler attached on a SBE 917 plus CTD (conductivity-temperature-depth; Sea-Bird Electronics Inc). Seawater samples of about 100 mL were collected at a depth of 5 m at each station and poisoned with 50 μL of saturated $HgCl_2$ solution immediately. The seawater sampling sites and their detailed sampling information are given in Table 2 and plotted in Figure 1. Seawater temperature (ºC) and salinity (psu) values were derived using the software package SBE Data Processing-Win32.

https://doi.org/10.1017/RDC.2018.100 Published online by Cambridge University Press

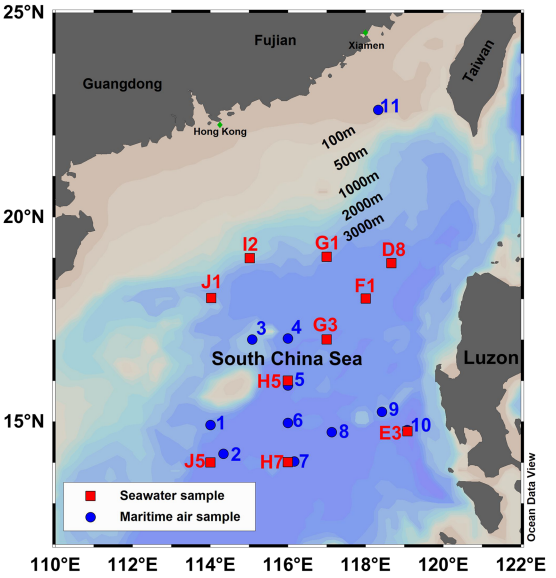

Figure 1 Sampling sites for maritime air and sea surface water in the SCS during the cruise in 2014. The letters of the seawater samples were names of different sections (from A to J) which followed the experimental design of the cruise in 2014; while the air samples stations were simply named after their sampling sequence.

^{14}C Analysis

Both air and seawater samples were processed for ^{14}C analysis at the Cosmogenic Nuclide Sample Preparation Laboratory of the Key Laboratory for Earth Surface Processes in Peking University, China. Atmospheric CO_2 was cryogenically purified on a vacuum line and then graphitized with the sealed-tube Zn reduction method (Xu et al. 2007). DIC from seawater

Table 1 Sampling information and ^{14}C results of the SCS atmospheric CO_2. The ^{14}C uncertainties are the analytical errors from individual measurements.

Station	Sampling time	Latitude (°N)	Longitude (°E)	Wind speed (m/s)	Wind direction (°)	$F^{14}C$	±	$\Delta^{14}C$ (‰)	± (‰)
1	20140706 09:00	14.914	114.004	7.3	245	1.0283	0.0020	20.3	2.0
2	20140707 17:05	14.211	114.338	7.5	247	1.0296	0.0017	21.7	1.7
3	20140709 10:50	17.006	115.080	3.4	196	1.0249	0.0015	17.0	1.5
4	20140709 18:52	17.030	116.002	4.8	171	1.0282	0.0016	20.3	1.6
5	20140710 07:42	15.880	116.000	7.2	206	1.0235	0.0016	15.6	1.6
6	20140710 17:18	14.965	115.999	7.6	212	1.0242	0.0015	16.3	1.5
7	20140711 03:32	14.025	116.160	7.1	201	1.0265	0.0015	18.6	1.5
8	20140711 19:13	14.741	117.127	6.3	175	1.0299	0.0016	22.0	1.6
9	20140713 21:50	15.236	118.426	3.7	202	1.0294	0.0016	21.4	1.6
10	20140715 00:25	14.790	119.078	4.2	295	1.0249	0.0016	17.0	1.6
11	20140717 18:00	22.615	118.326	8.1	72	1.0161	0.0015	8.3	1.5

https://doi.org/10.1017/RDC.2018.100 Published online by Cambridge University Press

Table 2 Sampling information and ^{14}C results of the SCS surface water DIC. The ^{14}C uncertainties are the analytical errors from individual measurements.

Station	Sampling time	Latitude (°N)	Longitude (°E)	Depth (m)	Salinity (psu)	Temperature (°C)	$F^{14}C$	±	$\Delta^{14}C$ (‰)	± (‰)
I2	20140620 19:07	18.993	115.017	5	33.55	29.52	1.0388	0.0022	30.8	2.2
G1	20140621 12:25	19.022	117.002	5	33.68	29.42	1.0475	0.0024	39.5	2.4
D8	20140625 14:32	18.865	118.666	5	33.55	29.34	1.0487	0.0027	40.6	2.7
F1	20140626 00:43	18.001	118.006	5	33.33	29.37	1.0450	0.0027	37.0	2.7
J1	20140629 19:37	18.017	114.025	5	33.40	30.56	1.0426	0.0017	34.6	1.7
J5	20140706 23:17	13.999	114.003	5	33.37	29.81	1.0395	0.0029	31.5	2.9
H5	20140710 03:06	16.000	116.000	5	33.11	29.73	1.0379	0.0041	29.9	4.1
H7	20140711 00:39	14.004	116.001	5	33.39	29.45	1.0363	0.0025	28.3	2.5
G3	20140712 19:34	17.003	117.002	5	33.15	30.27	1.0403	0.0022	32.3	2.2
E3	20140714 16:00	14.760	119.085	5	33.13	30.33	1.0481	0.0025	40.0	2.5

samples was extracted using the headspace-extraction method (Gao et al. 2014) from a volume of 30 mL after acidification with H_3PO_4, and then purified and graphitized in the same way as the CO_2 samples. Graphite samples were pressed into aluminum targets and measured for ^{14}C at Peking University Accelerator Mass Spectrometry (PKUAMS) facility (Liu et al. 2007).

All ^{14}C results discussed in the text are expressed as the per mil deviation ($\Delta^{14}C$) from 95% of the NBS oxalic acid I (OX-I) activity in 1950 as defined by Reimer et al. (2004) (with the age correction back to the sampling year), and are fractionation corrected to –25‰ using the online $^{13}C/^{12}C$ measurements in the AMS system which account for all potential fractionations occurred during the laboratory procedures and AMS measurements. For future reference, the ^{14}C results are also presented as fraction modern ($F^{14}C$) in Tables 1 and 2. The precision of $\Delta^{14}C$ measurements for modern samples is ~3‰ based on long-term measurements of secondary standards, such as OX-II, IAEA-C6, IAEA-C2, and CSTD-Coral. The ^{14}C uncertainties reported in this study are mainly the counting statistical errors from individual AMS measurements but adjusted based on the precisions of the six OX-I standards measured in the same wheel.

RESULTS

$^{14}CO_2$ over the SCS

The $\Delta^{14}C$ values of 11 individual maritime air samples are listed in Table 1 and plotted in Figure 2 (left). The average $\Delta^{14}C$ of the central SCS maritime air was 19.0 ± 2.4‰ (1 σ stdev, n = 10), with a range from 15.6 ± 1.6‰ to 22.0 ± 1.6‰. Samples collected from sites close to one another on the same day (e.g., Stations 3 and 4, 5 and 6, 7 and 8) yielded $\Delta^{14}C$ values in excellent agreement with each other (17.0 ± 1.5‰ and 20.3 ± 1.6‰; 15.6 ± 1.6‰ and 16.3 ± 1.5‰; 18.6 ± 1.5‰ and 22.0 ± 1.6‰), indicating that the sampling procedure and measurements were robust. Station 11, located next to the continental margin of Southeastern China, showed a much depleted $\Delta^{14}C$ value of 8.3 ± 1.5‰, which was ~10‰ lower than the central SCS maritime air $\Delta^{14}C$ values.

DI^{14}C of Surface Seawater in the SCS

The $\Delta^{14}C$ values of 10 individual surface seawater samples are listed in Table 2 and plotted in Figure 2 (right). They varied between 28.3 ± 2.5‰ and 40.6 ± 2.7‰, with an average of 34.4 ± 4.5‰ (1 σ stdev, n = 10). Stations E3 and D8, which are located in the easternmost part

https://doi.org/10.1017/RDC.2018.100 Published online by Cambridge University Press

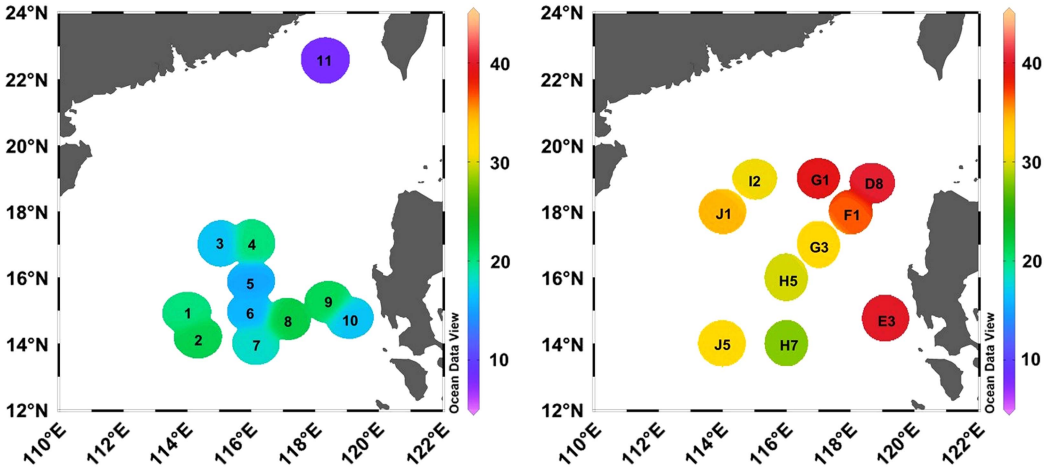

Figure 2 $\Delta^{14}C$ distributions of maritime air CO_2 (left) and surface seawater DIC (right) of the SCS.

of the sampling area, displayed the highest $\Delta^{14}C$ values of about 40‰ among all stations. The lowest $\Delta^{14}C$ values (29.9‰ and 28.3‰ at Stations H5 and H7, respectively) were observed in the central SCS along the 116°E section. Mid-range $\Delta^{14}C$ values of 31.5‰ and 34.6‰ were observed at stations J5 and J1, respectively, in the western part of the study area.

DISCUSSION

$\Delta^{14}C$ Spatial Variations and their Controls

The temporary wind direction varied between 171° and 295° and the wind speed was between 3.4 and 7.6 m/s at the time of maritime air sampling in the central SCS (excluding Station 11), indicating that the area was mainly influenced by strong southwest wind during the period of July 6–15, 2014. In order to show the air mass source and transport route for a longer time, backward trajectory plot (Figure 3) derived from the NOAA HYSPLIT model (Draxler and Rolph 2013) was conducted for the last 24 hr for each sampling site. Air masses arriving Stations 1–8 were basically originated from the southwestern open ocean area and underwent long distance transport. For Station 9, the air mass source shifted to the south and the transport route was relatively short; while Station 10 seemed to be influenced by local air mass since the transport route was confined in a very small area. The results of the back trajectory analysis revealed that most of the central SCS were dominated by air mass from the southwest.

The $\Delta^{14}CO_2$ spatial variation range was ~6‰ (comparable to the measurement uncertainty) and the average $\Delta^{14}C$ value was 19.0 ± 2.4‰ ($n = 10$) for Stations 1–10, indicating that the maritime air mass in central SCS was very well mixed. The SCS $\Delta^{14}CO_2$ value was also in excellent agreement with the atmospheric $\Delta^{14}CO_2$ recorded in Barrow, AK, which were 19.1 ± 2.3‰ ($n = 6$) in June and 21.1 ± 1.7‰ ($n = 3$) in July 2014 (X. Xu, unpublished data). Such a consistency between the SCS oceanic sites and the Alaskan coastal site points to a well-mixed and clean open ocean air background of $^{14}CO_2$ at the SCS.

The sample from Station 11, located on the northeastern continental shelf of the SCS (~200 km away from Xiamen; water depth < 50 m), showed a depleted $\Delta^{14}C$ value compared to the rest of the maritime air samples. The wind direction shifted to the east (72°) and the wind speed was particularly strong (8.1 m/s) during sampling. The backward air mass trajectories (Figure 3)

https://doi.org/10.1017/RDC.2018.100 Published online by Cambridge University Press

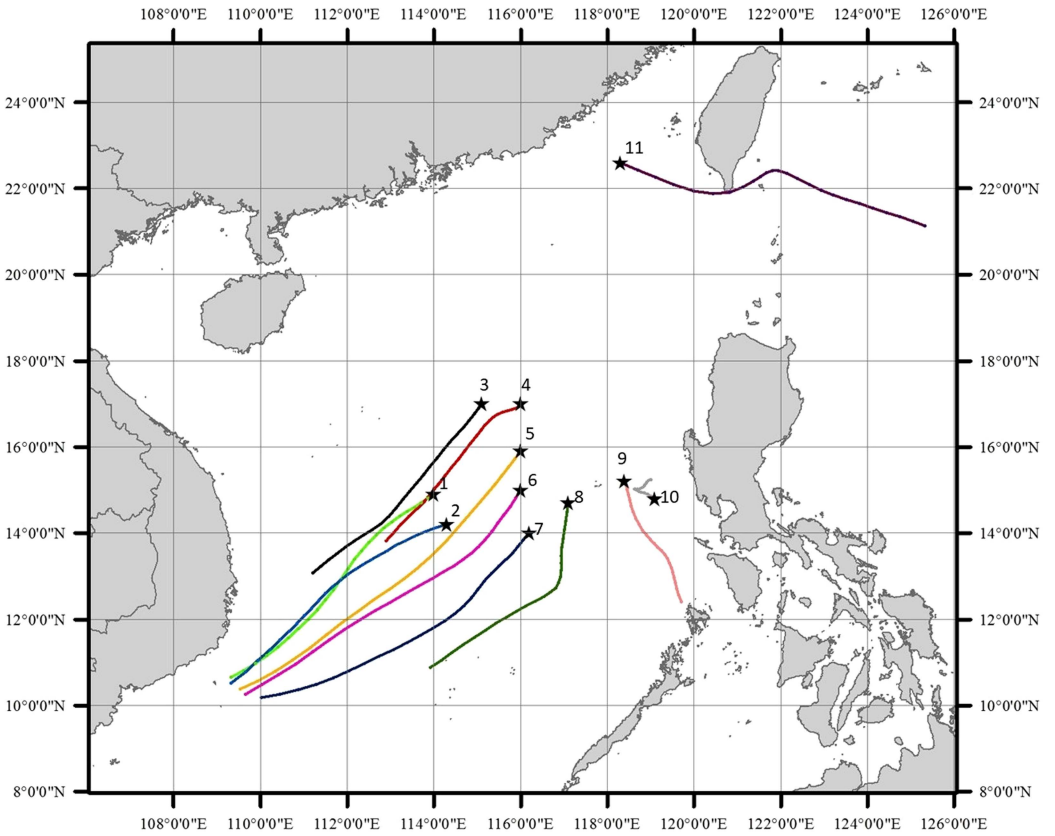

Figure 3 Twenty-four hours air mass back trajectories at 10 m above sea level of the 11 maritime air sampling sites, derived from the NOAA HYSPLIT (Hybrid Single-Particle Lagrangian Integrated Trajectory) Model (http://ready.arl.noaa.gov/HYSPLIT.php).

also suggest that this station was influenced by air mass originated from the east. The differences in wind direction and source regions at this station likely explain the $\Delta^{14}C$ depletion, indicating that air masses from the east experienced a dilution of anthropogenic ^{14}C-free CO_2 from the fossil fuel emission when passing over Taiwan. A rough calculation based on a simple two-end member mixing suggests that the fraction of fossil fuel CO_2 would be ~1% at Station 11, assuming fossil fuel CO_2 with $\Delta^{14}C$ of –995‰ and the clean maritime CO_2 with a $\Delta^{14}C$ of ~19‰.

During June–July 2014, surface seawater samples collected in the central SCS (Stations H5 and H7) showed the lowest $\Delta^{14}C$ values among all the stations. From 116º to 120ºE, surface seawater $\Delta^{14}C$ increased along the longitude and showed the highest values in the easternmost stations next to Luzon. The $\Delta^{14}C$ spatial variation range of the SCS surface seawater was ~12‰, which was larger than that of the maritime air in the same region. Besides air–sea exchange processes, other mechanisms such as vertical mixing between surface and subsurface water and/or lateral exchange between different water masses might also be responsible for the observed $\Delta^{14}C$ spatial difference.

Since the bomb ^{14}C perturbation has been several decades old and the air–sea gradients in ^{14}C have become substantially smaller, Graven et al. (2012) proposed that the changes in global

https://doi.org/10.1017/RDC.2018.100 Published online by Cambridge University Press

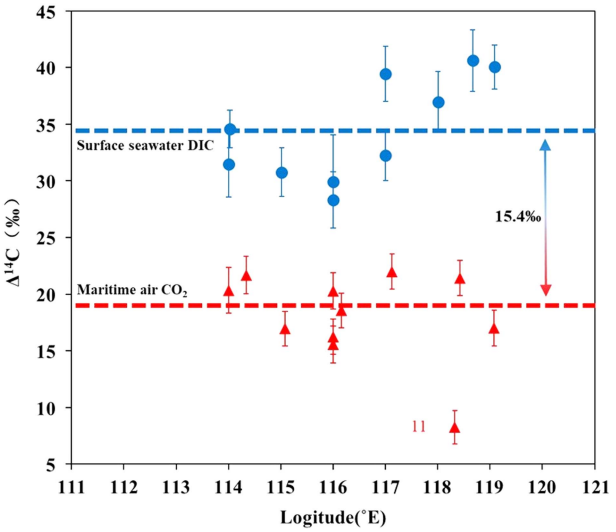

Figure 4 $\Delta^{14}C$ difference between the SCS maritime air CO_2 (red triangle) and sea surface water DIC (blue circles). Red and blue dashed lines denote the average $\Delta^{14}C$ values of maritime air CO_2 (excluding Station 11) and sea surface water DIC, respectively.

upper layer oceanic ^{14}C are now primarily controlled by shallow-to-deep water (or surface to subsurface) exchange. Inside the SCS basin, vertical mixing induced by physical oceanographic processes such as eddies and internal waves are relatively strong in the Luzon Strait and the continental shelves but relatively weak in the central SCS (Tian et al. 2009; Zhang et al. 2016). If the surface to subsurface water exchange induced by vertical mixing were the dominant control, the surface water of Luzon Strait and the continental shelves of the SCS would display more depleted $\Delta^{14}C$ values compared to those of the central SCS. However, the most depleted surface water $\Delta^{14}C$ values were recorded in the central SCS. Hence vertical mixing cannot explain the surface water $\Delta^{14}C$ spatial difference observed in the SCS. Other mechanism(s) must be considered.

Compared to the open ocean condition in the western Pacific, the surface water of the SCS is very well mixed with the subsurface water due to overall enhanced vertical mixing in this marginal sea (Tian et al. 2009). The surface water $\Delta^{14}C$ was 28.3–40.6‰ for the SCS and nearly constant for most of the stations in the upper 150 m (L. Zhou and P. Gao, unpublished data). Furthermore, the surface water of the western Pacific collected in the east of Luzon Strait along the 123ºE transect (sampled on May 27–29, 2014, during the same cruise) had higher $\Delta^{14}C$ (39.1–43.6‰) because it did not mix readily with the subsurface waters, and there was usually a subsurface $\Delta^{14}C$ maximum (46.4–55.6‰) at depths of around 200 m (L. Zhou and P. Gao, unpublished data). Thus, we attribute the spatial difference in the SCS observed here to the horizontal exchange between the SCS and the western Pacific. Stations in the easternmost part of the sampling area were influenced by the high $\Delta^{14}C$ surface water masses from the western Pacific surface waters, probably through the invasion of Kuroshio Current. Although there are some seasonal and inter-annual variations, the horizontal intrusion of western Pacific water through Luzon Strait makes important contribution to the water properties in the upper layer and regulates the surface circulation patterns in the northeastern SCS (Qu 2002; Li and Qu 2006; Tian et al. 2006; Yang et al. 2010; Hsin et al. 2012; Nan et al. 2015). In our sampling

https://doi.org/10.1017/RDC.2018.100 Published online by Cambridge University Press

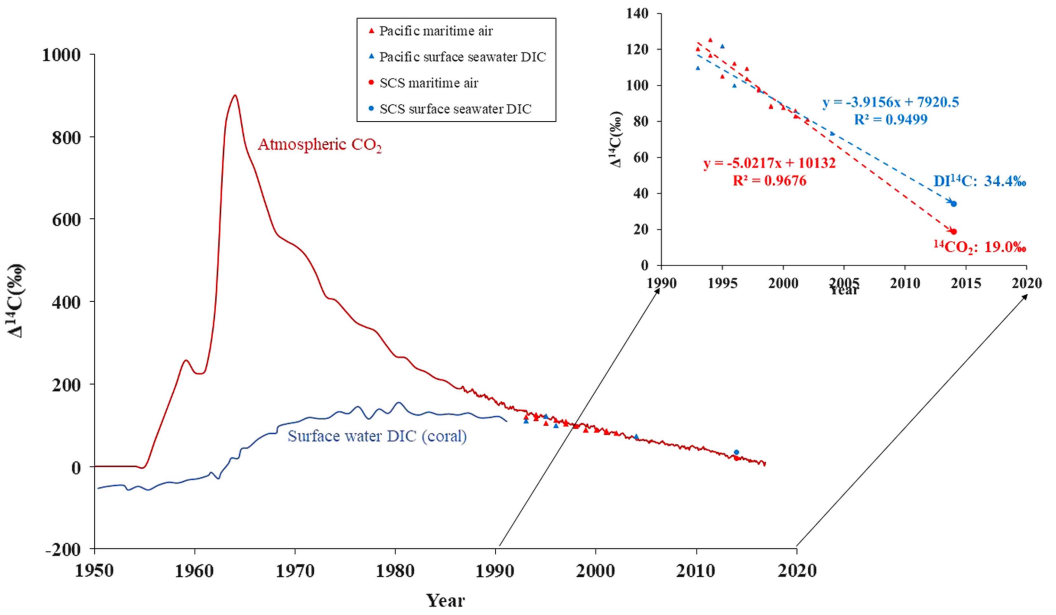

Figure 5 Decreasing trend of bomb ^{14}C in the air of the mid-latitudes in the Northern Hemisphere (red curve, Levin and Kromer 2004; Levin et al. 2013; Hammer and Levin 2017) and in surface water DIC derived from corals around 23ºS in the Pacific Ocean (blue curve, Druffel and Suess 1983; Druffel and Griffin 1995). Annual averaged $\Delta^{14}C$ values of Pacific maritime air CO_2 between 17ºS–28ºN from Kitagawa et al. (2004) and surface water $DI^{14}C$ data between 0–35ºN and 130–150ºE from GLODAP database (Key et al. 2004) are marked as red and blue triangles, respectively; SCS maritime air $^{14}CO_2$ and sea surface water $DI^{14}C$ from this study are marked with red and blue circles.

season, the surface circulation driven by the southwest wind was mainly anti-cyclonic, which would have prevented further invasion of the high $\Delta^{14}C$ western Pacific surface waters to the stations west of 118ºE.

$\Delta^{14}C$ Difference between Air and Surface Seawater and Its Implications

The measured $\Delta^{14}C$ values of the maritime air over the SCS were compared with that of the sea surface water in Figure 4. The average sea surface water $DI^{14}C$ value was 15.4 ± 5.1‰ higher than that of the $^{14}CO_2$ of central SCS maritime air (excluding Station 11). This was due to both the addition of the ^{14}C-free fossil fuel emission to the atmosphere and the increased bomb ^{14}C accumulation in surface ocean during the past decades (Suess 1955; Graven et al. 2012).

The ^{14}C in the air–sea interface is particularly useful for extrapolating CO_2 gas exchange parameterizations (Toggweiler et al. 1989; Krakauer et al. 2006; Sweeney et al. 2007). Several investigations have been conducted to derive the sea–air CO_2 fluxes in the SCS (Dai et al. 2013; Zhai et al. 2013). The $\Delta^{14}C$ in the SCS maritime air and surface seawater can help further constrain the air–sea exchange rate and assess the potential ability of the SCS as a natural and anthropogenic CO_2 source or sink.

Overall, the low latitude coastal systems outgas CO_2 due to the high temperature, high pCO_2 and high terrestrial organic carbon (OC) input. Dai et al. (2013) and Zhai et al. (2013) showed that most areas of the SCS served as weak to moderate sources of the atmospheric CO_2, and in

https://doi.org/10.1017/RDC.2018.100 Published online by Cambridge University Press

summer the source term was more significant than that in other seasons. In our sampling season, the surface ocean of the SCS would be expected to act as a CO_2 source, outgassing high ^{14}C to the atmosphere and causing some increase of maritime air ^{14}C in the region. However, there were seasonal changes and even reversal from source to sink in the SCS in regions such as the area off the Pearl River estuary (Zhai et al. 2013). In such areas, the surface ocean might become a CO_2 sink, and the absorption of ^{14}C-depleted maritime air CO_2 could induce the lower ^{14}C into the surface water layer.

Nevertheless, as a marginal sea, the SCS has very active upper layer vertical mixing; coastal upwelling might bring water to the surface and liberate CO_2 to the atmosphere. The $\Delta^{14}C$ of the upwelling water depends on the depth of the water source; upwelled subsurface water has the similar high $\Delta^{14}C$ values as the surface water, while upwelled deep water with depleted $\Delta^{14}C$ will cause a decrease in surface water $\Delta^{14}C$. Such processes may have a positive or negative effect on the maritime air $^{14}CO_2$ through air–sea exchange processes.

Temporal Trends of the Air and Surface Seawater $\Delta^{14}C$

By comparing to the historical data, Figure 5 illustrates the temporal change in atmospheric $^{14}CO_2$ and surface seawater $DI^{14}C$ since 1950. During the period of pre-1957, ^{14}C of atmospheric CO_2 stayed close to 0‰ (natural atmospheric ^{14}C level at the time). As the equilibration timescale (~10 yr; Broecker and Peng 1974) of $^{14}C/^{12}C$ ratio between the surface ocean and the CO_2 in the overlying air is longer than the residence time of water in the surface mixed layer, the ^{14}C level of DIC in the surface ocean is far from equilibrium with the atmosphere. Measurements of coral carbonate pre-1957 showed that surface water DIC averaged around −50‰ (Druffel and Suess 1983), which gave a mean marine surface reservoir age of ~400 yrs. After the thermonuclear weapons testing, the ^{14}C content of tropospheric CO_2 peaked to a level of ~840‰ in the Northern Hemisphere by 1964, and then decreased quasi-exponentially in the following decades to about 31.5 ± 2.0‰ in 2012 (Levin et al. 2013). Before the 1990s, the decline of the tropospheric $^{14}CO_2$ was mainly caused by the exchange of bomb ^{14}C with the stratosphere and with the ocean and the terrestrial biosphere, but subsequently was increasingly controlled by the input of ^{14}C-free fossil fuel derived CO_2 (Levin et al. 2010). The bomb ^{14}C entered the ocean and the surface water $DI^{14}C$ increased to about 130‰ by 1974 (Druffel and Griffin 1995), while the sea–air $\Delta^{14}C$ gradients reached a value of around –300‰ at the same time. As the bomb ^{14}C inventory had built up continuously in the upper ocean, the sea–air $\Delta^{14}C$ gradients decreased to the pre-bomb level of –50‰ in the late 1980s and became substantially smaller in 1990s (Figure 5). The western Pacific maritime air $^{14}CO_2$ (Kitagawa et al. 2004) and surface water $DI^{14}C$ (Key et al. 2004) had approached about the same value in the late 1990s. By 2014, the modern sea–air $\Delta^{14}C$ gradient in the SCS showed a positive value of 15.4‰ (Figures 4 and 5), the upper ocean has now becoming a source of bomb ^{14}C and is capable of transferring ^{14}C back to the atmosphere.

The red and blue dashed line in Figure 5 represent the linear regression trends of maritime air $^{14}CO_2$ and surface seawater $DI^{14}C$ from the 1990s, respectively. Comparing to the historical data from western Pacific, an average $\Delta^{14}C$ decline rate of 5.0‰ per year from 1994 to 2014 was obtained for maritime air, which was compatible to the global trend since the SCS air samples have the same $^{14}CO_2$ as the continental background station in Alaska. For surface seawater $DI^{14}C$, a decreasing rate of 3.9‰ per year from 1993 to 2014 was obtained at 14–17°N in the SCS. This rate may be slightly higher than the global trend, as the SCS has relatively lower surface seawater $DI^{14}C$ compared to the open ocean of western Pacific. The maritime air $^{14}CO_2$ has decreased faster than the surface seawater $DI^{14}C$, mainly due to the

https://doi.org/10.1017/RDC.2018.100 Published online by Cambridge University Press

large size of oceanic carbon reservoir and the dilution of ^{14}C free CO_2 from fossil fuel emission to the atmosphere in the past decades. The crossover of the two $\Delta^{14}C$ decline trend lines pointed to a reversal from negative to positive sea–air $\Delta^{14}C$ gradient at around 2000 in this region (Figure 5).

In the past decades, human-induced bomb ^{14}C has served as an useful tracer to study the carbon exchange between different reservoirs. However, it also introduces ambiguity for conventional radiocarbon dating since at least two samples have to be measured to determine whether the sample was on the increasing or declining side of the bomb curve. The reversal of sea–air $\Delta^{14}C$ gradient from negative to positive will add more complication to the reservoir age/residence time of surface water because the gradient is highly depended on the locality of ocean regime, even in the pre-bomb period (Alves et al. 2018). In the following decades when $F^{14}C$ of atmospheric CO_2 decreases to less than 1, prior and post bomb samples will no longer be distinguishable by radiocarbon measurement alone. Other proxies such as stable carbon isotope have to be measured for assistance (Köhler 2016). The $\Delta^{14}C$ features of global/local carbon reservoirs will change substantially because of the continuous fossil fuel emissions and the release of accumulated bomb ^{14}C in the upper oceans, not only in the mid ocean gyres, but also in some marginal seas such as the SCS that are weak to moderate CO_2 sources. More observations should be made on the spatial and temporal variation of sea–air $\Delta^{14}C$ gradient, as air–sea gas exchange is not a uniform process over the global oceans, but highly dependent on the local ocean dynamics.

CONCLUSIONS

In this study, we obtained the first records of ^{14}C in the air and surface seawater over the SCS, covering the latitudes of 14–17ºN and longitudes of 114–119ºE. The $\Delta^{14}C$ values of the atmospheric CO_2 and the seawater DIC varied in the ranges of $15.6 \pm 1.6‰$ to $22.0 \pm 1.6‰$ and $28.3 \pm 2.5‰$ to $40.6 \pm 2.7‰$, respectively. The $\Delta^{14}C$ signature of the maritime air in the SCS was consistent with the clean background air in the Northern Hemisphere except for one station on the northeastern continental shelf of the SCS where noticeable fossil fuel CO_2 contribution was observed. There was an eastward increase in ^{14}C value of the seawater DIC, which we attributed to the lateral seawater exchange between the SCS and western Pacific. The sea–air $\Delta^{14}C$ gradient in the SCS reached $15.4 \pm 5.1‰$ in 2014; higher bomb ^{14}C was documented in the surface ocean of this region, thus indicating the possibility of a bomb ^{14}C transfer from the ocean back to the atmosphere. By comparing the present SCS with the 1990s data from the Pacific, decline rates of 5.0‰ and 3.9‰ per year were obtained for maritime air $^{14}CO_2$ and surface seawater $DI^{14}C$ respectively in this region. It is hoped that more paired measurements of ^{14}C for surface seawater and the air above, together with other seawater DIC concentration/pCO_2 data, will serve as a useful tool for constraining the air–sea exchange processes as well as ocean circulation processes in the SCS.

ACKNOWLEDGMENTS

This study was funded by the National Natural Science Foundation of China (No. 91228209) and China Postdoctoral Science Foundation (No. 2015M570889), as well as the 111 Project (B14001). We thank the captain and crew of the R/V *Dongfanghong 2* for their assistance and Prof. Shao Min and Lu Sihua for providing the air sampling canisters. We also thank Dr. Zhang Jingcan, Shuai Geiwei, and Huang Tianyi for their help during the onboard sampling, and Qin Xiaoxin for advice on the use of the NOAA HYSPLIT model.

REFERENCES

Alves EQ, Macario K, Ascough P, Bronk Ramsey C. 2018. The worldwide marine radiocarbon reservoir effect: definitions, mechanisms, and prospects. *Reviews of Geophysics* 56:278–305.

Bhushan R, Krishnaswami S, Somayajulu BLK. 1997. ^{14}C in air over the Arabian Sea. *Current Science* 73(3):273–6.

Broecker WS, Peng TH. 1974. Gas exchange between air and sea. *Tellus* 26(1–2):21–35.

Broecker WS, Peng TH, Ostlund G, Stuiver M. 1985. The distribution of bomb radiocarbon in the ocean. *Journal of Geophysical Research* 90:6953–70.

Broecker WS, Patzert WC, Toggweiler JR, Stuiver M. 1986. Hydrography, chemistry, and radioisotopes in the Southeast Asian basins. *Journal of Geophysical Research Oceans* 91(C12):14345–54.

Caldeira K, Rau GH, Duffy PB. 1998. Predicted net efflux of radiocarbon from the ocean and increase in atmospheric radiocarbon content. *Geophysical Research Letters* 25(20):3811–4.

Centurioni LR, Niiler PP, Lee D K. 2004. Observations of Inflow of Philippine Sea Surface Water into the South China Sea through the Luzon Strait. *Journal of Physical Oceanography* 34:113–21.

Dai M, Cao Z, Guo X, Zhai W, Liu Z, Yin Z, Xu Y, Gan J, Hu J, Du C. 2013. Why are some marginal seas sources of atmospheric CO_2? *Geophysical Research Letters* 40(10):2154–8.

Draxler RR, Rolph GD. 2013. HYSPLIT (HYbrid Single-Particle Lagrangian Integrated Trajectory) Model access via NOAA ARL READY Website (http: //www.arl.noaa.gov/ HYSPLIT.php). NOAA Air Resources Laboratory, College Park, MD.

Druffel ERM, Suess HE. 1983. On the radiocarbon record in banded corals: Exchange parameters and net transport of $^{14}CO_2$, between atmosphere and surface ocean. *Journal of Geophysical Research Oceans* 88(C2):1271–80.

Druffel ERM, Griffin S. 1995. Regional variability of surface ocean radiocarbon from southern Great Barrier Reef corals. *Radiocarbon* 37(2):517–24.

Dutta K. 2002. Coherence of tropospheric $^{14}CO_2$ with El Niño/Southern Oscillation. *Geophysical Research Letters* 29(20):1987.

Dutta K, Bhushan R, Somayajulu BLK, Rastogi N. 2006. Inter-annual variation in atmospheric $\Delta^{14}C$ over the Northern Indian Ocean. *Atmospheric Environment* 40(24):4501–12.

Fang G, Wang Y, Wei Z, Fang Y, Qiao F, Hu X, 2009. Interocean circulation and heat and freshwater budgets of the South China Sea based on a numerical model. *Dynamics of Atmospheres and Oceans* 47:55–72.

Gan J, Li H, Curchitser EN, Haidvogel DB. 2006. Modeling South China Sea circulation Response to seasonal forcing regimes. *Journal of Geophysical Research* 111:C06034.

Gao P, Xu X, Zhou L, Pack MA, Griffin S, Santos GM, Southon JR, Liu K. 2014. Rapid sample preparation of dissolved inorganic carbon in natural waters using a headspace-extraction approach for radiocarbon analysis by accelerator mass spectrometry. *Limnology & Oceanography Methods* 12(4):174–90.

Graven HD, Gruber N, Key RM, Khatiwala S, Giraud X. 2012. Changing controls on oceanic radiocarbon: New insights on shallow-to-deep ocean exchange and anthropogenic CO_2 uptake. *Journal of Geophysical Research Oceans* 117(C10): 005.

Hammer S, Levin I. 2017. Monthly mean atmospheric $D^{14}CO_2$ at Jungfraujoch and Schauinsland from 1986 to 2016. heiDATA Dataverse, V2. doi:10.11588/data/10100.

Hsin YC, Wu CR, Chao SY. 2012. An updated examination of the Luzon Strait transport. *Journal of Geophysical Research Oceans* 117: C03022.

Key RM, Kozyr A, Sabine CL, Lee K, Wanninkhof R, Bullister JL, Feely RA, Millero FJ, Mordy C, Peng TH. 2004. A global ocean carbon climatology: Results from Global Data Analysis Project (GLODAP). *Global Biogeochemical Cycles* 18 (4):357–70.

Kitagawa H, Mukai H, Nojiri Y, Shibata Y, Kobayashi T, Nojiri T. 2004. Seasonal and secular variations of atmospheric $^{14}CO_2$ over the Western Pacific since 1994. *Radiocarbon* 46(2):901–10.

Köhler P. 2016. Using the Suess effect on the stable carbon isotope to distinguish the future from the past in radiocarbon. *Environmental Research Letters* 11:124016.

Krakauer NY, Randerson JT, Primeau FW, Gruber N, Menemenlis D. 2006. Carbon isotope evidence for the latitudinal distribution and wind speed dependence of the air–sea gas transfer velocity. *Tellus B: Chemical & Physical Meteorology* 58(5):390–417.

Levin I, Kromer B. 2004. The Tropospheric $^{14}CO_2$ level in mid-latitudes of the Northern Hemisphere (1959–2003). *Radiocarbon* 46(3):1261–72.

Levin I, Naegler T, Kromer B, Diehl M, Francey RJ, Gomez-Pelaez AJ, Steele LP, Wagenbach D, Weller R, Worthy DE. 2010. Observations and modelling of the global distribution and long-term trend of atmospheric $^{14}CO_2$. *Tellus B* 62(1): 26–46.

Levin I, Kromer B, Hammer S. 2013. Atmospheric $\Delta^{14}CO_2$ trend in Western European background air from 2000 to 2012. *Tellus B: Chemical & Physical Meteorology* 65(1):20092.

Li L, Qu T. 2006. Thermohaline circulation in the deep South China Sea basin inferred from oxygen distributions. *Journal of Geophysical Research Oceans* 111(C05):017.

Liu K, Ding X, Fu D, Pan Y, Wu X, Guo Z, Zhou L. 2007. A new compact AMS system at Peking University. *Nuclear Instruments & Methods in Physics Research* 259(1):23–6.

https://doi.org/10.1017/RDC.2018.100 Published online by Cambridge University Press

Nan F, Xue H, Yu F. 2015. Kuroshio intrusion into the South China Sea: A review. *Progress in Oceanography* 137:314–33.

Qu T. 2000a. Upper-layer circulation in the South China Sea. *Journal of Physical Oceanography* 30:1450–60.

Qu T, Mitsudera H, Yamagata T. 2000b. Intrusion of the North Pacific waters into the South China Sea. *Journal of Geophysical Research* 105 (C3):6415–24.

Qu T. 2002. Evidence of water exchange between the South China Sea and the Pacific through the Luzon Strait. *Acta Oceanologica Sinica* 21 (2):175–85.

Reimer PJ, Thomas AB, Reimer RW. 2004. Discussion: reporting and calibration of post-bomb ^{14}C data. *Radiocarbon* 46(3):1299–304.

Shaw PT, Chao SY. 1994. Surface circulation in the South China Sea. *Deep-Sea Research I* 41:1663–83.

Su J. 2004. Overview of the South China Sea circulation and its influence on the coastal physical oceanography outside the Pearl River Estuary. *Continental Shelf Research* 24:1745–60.

Suess HE. 1955. Radiocarbon concentration in modern wood. *Science* 122(3166):415–7.

Sweeney C, Gloor E, Jacobson AR, Key RM, McKinley G, Sarmiento JL, Wanninkhof R. 2007. Constraining global air–sea gas exchange for CO_2 with recent bomb ^{14}C measurements. *Global Biogeochemical Cycles* 21:GB2015.

Tian J, Yang Q, Liang X, Xie L, Hu D, Wang F, Qu T. 2006. Observation of Luzon Strait transport. *Geophysical Research Letters* 33:L19607.

Tian J, Yang Q, Zhao W. 2009. Observation of enhanced diapycnal mixing in the South China Sea. *Journal of Physical Oceanography* 39 (12):3191–203.

Toggweiler JR, Dixon K, Bryan K. 1989. Simulations of radiocarbon in a coarse-resolution world ocean model: 1. Steady state prebomb distributions. *Journal of Geophysical Research Oceans* 94 (C6):8217–42.

Turnbull JC, Lehman SJ, Miller JB, Sparks RJ, Southon JR, Tans PP. 2007. A new high precision $^{14}CO_2$ time series for North American continental air. *Journal of Geophysical Research Atmospheres* 112(D11):310.

Wyrtki K. 1961. *Physical Oceanography of the Southeast Asian Waters. Naga Report 2*. La Jolla, California: Scripps Institute of Oceanography, University of California, San Diego. 195 p.

Xu X, Trumbore SE, Zheng S, Southon JR, McDuffe KE, Luttgen M, Liu JC. 2007. Modifying a sealed tube zinc reduction method for preparation of AMS graphite targets: Reducing background and attaining high precision. *Nuclear Instruments and Methods in Physics Research* 259(1):320–9.

Yang Q, Tian J, Zhao W. 2010. Observation of Luzon Strait transport in Summer 2007. *Deep-Sea Research I* 57(5):670–6.

Zhai W, Dai M, Chen B, Guo X, Li Q, Shang S, Zhang C, Cai W, Wang D. 2013. Seasonal variations of air–sea CO_2 fluxes in the largest tropical marginal sea (South China Sea) based on multiple-year underway measurements. *Biogeosciences* 10(11):7775–91.

Zhang Z, Tian J, Qiu B, Zhao W, Chang P, Wu D, Wan X. 2016. Observed 3D structure, generation, and dissipation of oceanic mesoscale eddies in the South China Sea. *Scientific Reports* 6:24349.